Separating a wavefield by propagation direction

Alan Richardson, formerly of Massachusetts Institute of Technology, and Alison E. Malcolm, Memorial University of Newfoundland*

SUMMARY

Determining the propagation direction of waves in a wavefield is important in several seismic imaging techniques and applications. This can be achieved using the Poynting vector method, but it performs poorly when waves overlap, returning incorrect wave amplitude and direction. An alternative, the local slowness method, is capable of separating overlapping waves, but suffers from low angular resolution. We describe modifications of these two approaches that improve the ability to extract the wave amplitude propagating in different directions. The primary modification is the addition of a wavefront orientation separation step. We evaluate the original and modified methods' ability to separate six overlapping waves in a constant velocity model and find that the modifications significantly improve the results.

INTRODUCTION

The propagation directions of waves can be used to construct Angle domain common image gathers (ADCIGs), which are used for velocity analysis (Biondi and Symes, 2004) and extracting Amplitude versus angle (AVA) information (Yan and Xie, 2012b), to attenuate backscatter artifacts in Reverse Time Migration (RTM) (Costa et al., 2009), and in illumination analysis (Yang et al., 2008). Several methods have been proposed for extracting directional information from finite-frequency wave propagation schemes. One of these is the Poynting vector method (Yoon and Marfurt, 2006), which is computationally efficient, but makes the assumption that the wavefield does not contain overlapping waves propagating in different directions. Another is the local slowness method (Xie et al., 2005), which does allow overlapping waves, but suffers from low angular resolution. In this paper we propose modifications of these two methods to improve these deficiencies.

We start by describing the Poynting vector and local slowness methods. Following this, we explain the modifications that we propose to apply to them, primarily consisting of the addition of a wavefront orientation separation step, to enhance the ability to separate overlapping waves. Finally, we examine the effectiveness of the new methods compared to the Poynting vector and local slowness methods.

PREVIOUSLY PROPOSED METHODS

In this section we describe the Poynting vector and local slowness methods for separating a wavefield by propagation direction.

Poynting vectors

The Poynting vector method of determining wave propagation direction was proposed by Yoon and Marfurt (2006) as a means of determining apparent scattering angle. It is not limited to calculating scattering angle, and so may also be used in applications where the propagation directions of the source and receiver wavefields must be known independently, such as in illumination compensation (Yang et al., 2008).

The Poynting vector method calculates the propagation direction $\hat{\psi}$ at a point $\mathbf{x}$ and time t of wavefield u using

$$\hat{\psi}(\mathbf{x},t;u) = -\frac{\partial u(\mathbf{x},t)}{\partial t}\nabla u(\mathbf{x},t)\left|\frac{\partial u(\mathbf{x},t)}{\partial t}\nabla u(\mathbf{x},t)\right|^{-1}. \quad (1)$$

The method assumes that there are no overlapping waves (Patrikeeva and Sava, 2013), so the method assigns the full amplitude at each point to a single propagation direction.

Local slowness

An alternative approach, called the local slowness method, was proposed by Xie et al. (2005). This method was initially developed to analyze near-source energy partitioning, but it has also been applied to determining propagation directions for illumination compensation (Xie and Yang, 2008) and constructing ADCIGs (Yan and Xie, 2012a). The method sums along local slowness directions in spacetime,

$$u_s(\mathbf{x},\mathbf{p},t) = \frac{1}{I_{\mathbf{x}}}\sum_{\mathbf{x}'} W(\mathbf{x}'-\mathbf{x})u(\mathbf{x}', t-\mathbf{p}\cdot(\mathbf{x}'-\mathbf{x})), \quad (2)$$

where u_s is the wavefield containing only waves propagating in the direction $\hat{\psi}$, $\mathbf{p}=\frac{\hat{\psi}}{c}$ is the slowness, and W is a space window of length $I_{\mathbf{x}}$ centered on $\mathbf{x}$. In contrast to the Poynting vector method, this approach is capable of separating a wavefield even when it contains overlapping waves propagating in different directions. The separation of overlapping waves is exact for plane waves in a constant velocity medium if the window W is sufficiently large, but when these assumptions aren't satisfied overlapping waves can still cause incomplete separation.

MODIFIED METHODS

In this section we propose modifications to the Poynting vector and local slowness methods. These primarily consist of preceding the methods by a separation of the

DOI http://dx.doi.org/10.1190/segam2015-5911824.1

wavefields by wavefront orientation, so we first discuss techniques by which this may be achieved. The proposed modification allows the Poynting vector method to separate overlapping waves and enhances the resolution of the local slowness method. We describe the methods in the 2D case for simplicity, however they may be extended to 3D without difficulty. We also assume that the wave propagation occurs in isotropic, non-attenuating media.

Wavefront orientation separation

The orientation of a wavefront, $\hat{\psi}$, is the direction of its gradient. In isotropic media, waves travel parallel to their wavefront orientation (i.e., the wavefront is perpendicular to the ray). A wavefront with orientation $\hat{\psi}$ must therefore belong to a wave propagating in the direction $\hat{\psi}$ or $-\hat{\psi}$. For locally planar waves, the wave amplitude is locally constant perpendicular to $\hat{\psi}$, and oscillatory parallel to it. In 2D we may refer to a wavefront of orientation $\hat{\psi}$ or $-\hat{\psi}$ as having orientation angle $\psi \in [0, \pi)$, where ψ is the angle from the positive x axis to whichever of $\hat{\psi}$ or $-\hat{\psi}$ lies in the positive z domain.

The separation into wavefront orientation angles can be accomplished by several means, including through the use of the Fourier transform, the Curvelet transform (Candès et al., 2006), and time domain Local slant stack (LSS). We describe only the last of these for conciseness.

Local slant stack

LSS uses the fact that locally planar waves are oscillatory perpendicular to the wavefront and approximately constant along it. Summing along a wavefront in space will yield a non-zero value. Any direction not parallel to the wavefront should sum to zero due to the oscillatory property, if the summation length is sufficiently long. If the time period over which the pulse is oscillatory (or almost oscillatory) is T, then the corresponding spatial length is $c(\mathbf{x})T$, where c is the wave speed, which we assume does not vary significantly over this distance. To make use of this property, we therefore need to sum along a wavefront over the distance $[-\frac{c(\mathbf{x})T}{2} : \frac{c(\mathbf{x})T}{2}]$ around the point $\mathbf{x}$ in order to prevent the calculated amplitude along a wavefront from being affected by a perpendicular wavefront also centered on $\mathbf{x}$. To avoid interference between wavefronts not perpendicular, or not centered on $\mathbf{x}$, we would need to sum over a larger distance. Our assumptions about the planar nature of the wavefront and the locally constant velocity are less likely to be valid at larger distances, however. Decomposing the wavefield into $N_s(t)$ equally spaced wavefront orientation angles (which will allow us to separate into $2N_s(t)$ propagation directions later) therefore requires a summation length of

$$I_{\mathbf{x}} = \frac{c(\mathbf{x})T}{\sin(\Delta\psi)}, \tag{3}$$

where

$$\Delta\psi = \frac{\pi}{N_s(t)}. \tag{4}$$

The angular resolution ($\Delta\psi$) obtainable with this method is approximately inversely proportional to $I_{\mathbf{x}}$ when $\Delta\psi$ is small. The maximum possible length $I_{\mathbf{x}}$ is determined by the smoothness of the model (in smooth models the length over which the approximations of the method are valid will be longer, and so a larger $I_{\mathbf{x}}$ can be used), so resolution is inversely proportional to model smoothness (a smoother model allows the separation of waves propagating in more closely spaced directions). Resolution is approximately proportional to $c(\mathbf{x})T$, the local wave speed and the shortest oscillatory time of the waves. Although it is a spatial quantity, in practice the summation length is often specified as the summation time I_t, as $I_{\mathbf{x}} = I_t c(\mathbf{x})$ varies in space with $c(\mathbf{x})$.

To separate the wavefield into waves with different wavefront orientation angles with LSS, we sum along different orientation angles at each point $\mathbf{x}$, and divide by the length of the sum to obtain the amplitude of the waves:

$$u_o(\mathbf{x}, \psi, t) = \sum_{s=-\frac{I_{\mathbf{x}}}{2}}^{\frac{I_{\mathbf{x}}}{2}} \frac{u(\mathbf{x} + s\hat{\psi}^{\perp}, t)}{I_{\mathbf{x}}}, \tag{5}$$

where $\hat{\psi}^{\perp}$ is the direction along a wavefront oriented with angle ψ (i.e., $\hat{\psi}^{\perp} = (-\sin(\psi)\hat{x}, \cos(\psi)\hat{z})$), u is the full wavefield, u_o is the scalar field containing the amplitude of waves with wavefront orientation angle ψ at position $\mathbf{x}$ and time t, and $I_{\mathbf{x}} = I_t c(\mathbf{x})$ is the summation length. If u is not defined at spatial locations requested by this summation, interpolation may be used.

As waves propagating in both the directions $\hat{\psi}$ and $-\hat{\psi}$ have wavefront orientation ψ, wavefront orientation separation alone cannot determine propagation directions.

Method 1: Modified Poynting vector method

We wish to determine the propagation directions and amplitudes of the $N(\mathbf{x}, t)$ waves passing through the point $\mathbf{x}$ at time t. If $\max(N) \leq 1$, the Poynting vector method works well and is computationally efficient, however it fails when $N > 1$.

In this modified method we separate the wavefield into waves with different wavefront orientations, and apply two filters, based on the Poynting vector method, to determine the propagation directions.

By separating the wavefield by orientation angle ψ, we hope that

$$max(N'(\mathbf{x}, \psi, t)) \leq 1, \tag{6}$$

where N' is the number of waves passing through the point $\mathbf{x}$ at time t that have a wavefront at point $\mathbf{x}$ oriented with angle ψ. If this condition is satisfied, then we may successfully apply the Poynting vector method for each direction $\hat{\psi}$ to determine the propagation amplitude in that direction. As wavefront orientation angle separation will not separate two overlapping waves propagating in opposite directions $\hat{\psi}$ and $-\hat{\psi}$, since both have the same wavefront orientation angle, the condition (6) can never be satisfied in this case. This method

DOI http://dx.doi.org/10.1190/segam2015-5911824.1

is therefore incapable of separating overlapping waves propagating in opposite directions.

Performing this separation on a sufficient number of time steps to calculate a time derivative (at least two), we calculate the Poynting vectors for each separated wavefront orientation, $\hat{\psi}_p(\mathbf{x},t;u_o(\mathbf{x},\psi,t))$, using Equation 1, and the apparent wave propagation speed using

$$c_a(\mathbf{x},\hat{\psi},t)=\left|\frac{\partial u_o(\mathbf{x},\psi,t)}{\partial t}\left(\frac{\partial u_o(\mathbf{x},\psi,t)}{\partial \hat{\psi}}\right)^{-1}\right|. \quad (7)$$

The calculated propagation speed will be incorrect near the peaks and troughs of the wave, as the spatial derivative at these locations will be close to zero, making the result unstable. We therefore smooth the calculated speed, weighted by the absolute value of the spatial derivative of $u_o(\mathbf{x},\psi,t)$.

Although the wavefront orientation angle ψ is in the range $[0,\pi)$, the wave propagation direction unit vector $\hat{\psi}$ covers the full circle because each ψ can produce a wave propagating in $\hat{\psi}$ or $-\hat{\psi}$. Both $\hat{\psi}_p$ and $-\hat{\psi}_p$ will therefore be computed using $u_o(\mathbf{x},\psi,t)$. The same applies to the calculation of $c_a(\mathbf{x},\hat{\psi},t)$.

If a wave is propagating in the direction $\hat{\psi}$, then $\hat{\psi}_p$ should point in the same direction if the medium is isotropic. We also know that the wave propagation speed should be $c(\mathbf{x})$. We exploit this to determine whether the wave with wavefront orientation angle ψ is propagating in the direction $\hat{\psi}$ or $-\hat{\psi}$, and to attenuate artifacts caused by violations of the method's assumptions. To achieve this, we calculate two filters. The first deals with the propagation direction,

$$filt_{ang}(\mathbf{x},\hat{\psi},t)=(1-\arccos(|\hat{\psi}_p\cdot\hat{\psi}|)/\pi)^d, \quad (8)$$

where d is a parameter to adjust how severely errors are treated. This expression computes the angular distance between the calculated propagation direction, $\hat{\psi}_p$, and the assigned propagation direction, $\hat{\psi}$, derived from the wavefront orientation. If the distance is zero, the filter has value 1. If the propagation direction is the opposite to the assigned direction, the filter has value 0.

For the second filter, we penalize departures of the apparent wave speed from the actual wave speed,

$$filt_c(\mathbf{x},\hat{\psi},t)=1-\min(|c(\mathbf{x},t)-c_a(\mathbf{x},\hat{\psi},t)|/maxerr,1), \quad (9)$$

where $maxerr$ is the maximum permissible error in c, for example 1000 m/s.

To obtain the wavefield separated by propagation direction, we multiply the wavefield separated by wavefront orientation with the two filters,

$$u_s(\mathbf{x},\hat{\psi},t)=u_o(\mathbf{x},\psi,t)filt_{ang}(\mathbf{x},\hat{\psi},t)filt_c(\mathbf{x},\hat{\psi},t). \quad (10)$$

Method 2: Modified local slowness

While the local slowness method is already capable of separating overlapping waves, preceding its application by a wavefront orientation step improves the achievable resolution.

Wavefront orientation separation has better resolution than the local slowness method for small differences in propagation direction, but its inability to distinguish between waves propagating in opposite directions means that it has poor resolution for large differences in propagation angle, the regime in which the resolution of the local slowness method is highest. By combining both methods we derive the benefits of wavefront orientation separation's good resolution at small angles while also retaining the local slowness method's ability to separate waves with large propagation angle differences.

If a wave, propagating in the direction $\hat{\psi}$, can be locally approximated by a plane wave, and the local wave speed is approximately constant, the wave travels along the path described by Equation 2 of the local slowness method. Furthermore, wavefronts along this path that are propagating in the direction $\hat{\psi}$ should have a wavefront orientation angle of ψ. To apply this last observation, we modify Equation 2 to use the output of wavefront orientation separation,

$$u_s(\mathbf{x},\hat{\psi},t)=\sum_{t'=-\frac{I_t}{2}}^{\frac{I_t}{2}}\frac{u_o(w(t',\mathbf{x},\psi,t),\psi,t')}{I_t}. \quad (11)$$

Including the wavefront orientation separation step increases the computational cost of the method compared to the original local slowness approach, but it improves the method's ability to distinguish between waves with small differences in propagation direction. This means that for the local slowness method to have sufficient resolution to separate such waves, the assumptions of the method must hold over a larger distance from the point being separated.

RESULTS

In this section we test the angular resolution under the idealized conditions of constant velocity. As the resolution of the summation-based approaches (the local slowness method and methods 1 and 2) is limited by the summation distance, we choose I_x for each method so that the maximum summation distance from the point being separated is the same for all of these methods.

In order to test the ability of the methods to separate overlapping waves, we create a wavefield using six sources arranged around a hemisphere of radius 750 m. The sources emit a 20 Hz Ricker wavelet, and the wave speed is constant everywhere at 1500 m/s. We attempt to separate the wavefield 0.5 s after the peak source input, as the six waves are crossing. The unseparated wavefield at this time is shown in Figure 1c. For method 1 and the local slowness method, we use 0.17 s, twice

DOI http://dx.doi.org/10.1190/segam2015-5911824.1

the duration of the source wavelet, as the summation time. According to Equation 3, this allows method 1 to separate waves with propagation directions differing by at least 30° (which is the minimum difference between waves in the example wavefield) without interference. For method 2 we use a summation time of 0.12 s.

In Figure 1 we show the amplitude of waves determined by different methods to be propagating in each direction at the chosen point, where the waves from the six sources are overlapping. As expected, the Poynting vector method fails in this test as its assumption that waves do not overlap is violated. The peak angle of the local slowness method is similar to that of the Poynting vector method (not visible in the displayed figures due to clipping), as the angular resolution with the given summation time is not sufficient to distinguish between the six propagation directions. Both of the modified methods produce results that are quite close to the true separation.

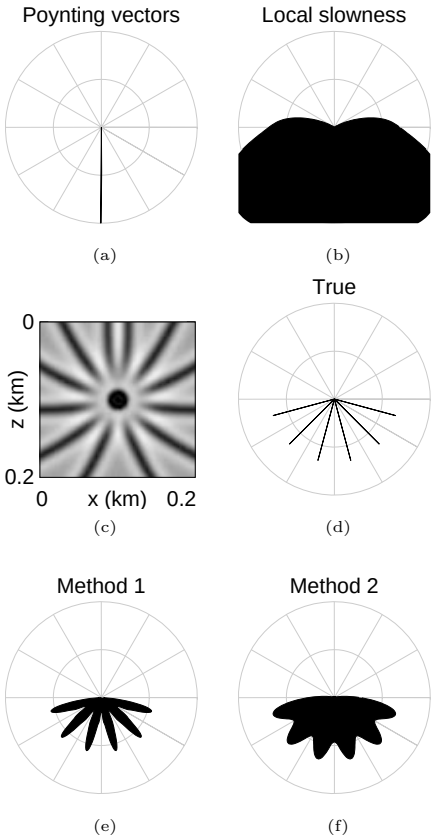

Figure 1: Results of directional separation. Propagation angle is on the polar axis, while the radial axis represents amplitude. The displayed amplitude range is the same for all polar plots. (c) shows a time slice of the central portion of the input wavefield with six waves overlapping obliquely.

To investigate the behavior of the methods under less idealized conditions, we consider the backpropagated receiver wavefield for a single shot in a 2D slice of the SEAM model (Fehler and Larner, 2008). We use a separation time of 0.266 s for the local slowness method and method 1, and 0.188 s for method 2.

As we do not know the true directional decomposition of this wavefield, we can only judge the results on how visually plausible they appear. One propagation direction (toward the bottom right) of the resulting separated wavefields at a single time step is shown in Figure 2. Figure 2a shows the full wavefield at this time step. Focusing on the effect of the overlapping wave A, we see that the low resolution of the local slowness method causes A to be clearly visible despite propagating in a different direction to that chosen. The overlapping wave A has a smaller impact on the output of the modified methods.

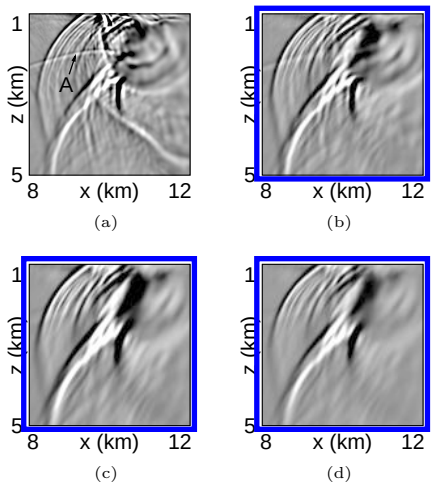

Figure 2: (a) Unseparated wavefield. (b) Local slowness method. (c) Method 1. (d) Method 2.

CONCLUSION

This paper presents modifications of the Poynting vector and local slowness methods for separating a wavefield into waves propagating in different directions. Unlike the previously proposed Poynting vector method, the modified version is capable of performing the separation even when there are overlapping waves. The local slowness method is also able to do this, but, as we demonstrate, it has poorer angular resolution than the modified version we propose. Separating the wavefield by wavefront orientation, a key component of both of our modified methods, provides good angular resolution, enabling them to separate six overlapping waves when both the Poynting vector and local slowness methods fail to do so.

ACKNOWLEDGMENTS

The authors wish to thank Total for support, and Paul Williamson of Total for his useful suggestions.

DOI http://dx.doi.org/10.1190/segam2015-5911824.1

EDITED REFERENCES

Note: This reference list is a copyedited version of the reference list submitted by the author. Reference lists for the 2015 SEG Technical Program Expanded Abstracts have been copyedited so that references provided with the online metadata for each paper will achieve a high degree of linking to cited sources that appear on the Web.

REFERENCES

Biondi, B., and W. W. Symes, 2004, Angle-domain common-image gathers for migration velocity analysis by wavefield-continuation imaging: Geophysics, **69**, 1283–1298. http://dx.doi.org/10.1111/j.1365-2478.2004.00444.x.

Candès, E., L. Demanet, D. Donoho, and L. Ying, 2006, Fast discrete curvelet transforms: Multiscale Modeling & Simulation, **5**, no. 3, 861–899. http://dx.doi.org/10.1137/05064182X.

Costa, J., F. Silva Neto, M. Alcântara, J. Schleicher, and A. Novais, 2009, Obliquity-correction imaging condition for reverse-time migration: Geophysics, **74**, no. 3, S57–S66. http://dx.doi.org/10.1190/1.3110589.

Fehler, M., and K. Larner, 2008, SEG Advanced Modeling (SEAM): Phase I first year update: The Leading Edge, **27**, 1006–1007.

Patrikeeva, N., and P. Sava, 2013, Comparison of angle decomposition methods for wave-equation migration: 83rd Annual International Meeting, SEG, Expanded Abstracts, 3773–3778.

Xie, X.-B., Z. Ge, and T. Lay, 2005, Investigating explosion source energy partitioning and Lg-wave excitation using a finite-difference plus slowness analysis method: Bulletin of the Seismological Society of America, **95**, no. 6, 2412–2427. http://dx.doi.org/10.1785/0120050023.

Xie, X.-B., and H. Yang, 2008, A full-wave equation based seismic illumination analysis method: Presented at the 70th Annual International Conference and Exhibition, EAGE.

Yan, R., and X.-B. Xie, 2012a, An angle-domain imaging condition for elastic reverse-time migration and its application to angle gather extraction: Geophysics, **77**, no. 5, S105–S115. http://dx.doi.org/10.1190/geo2011-0455.1.

Yan, R., and X.-B. Xie, 2012b, AVA analysis based on RTM angle-domain common image gather: Presented at the 82nd Annual International Meeting, SEG.

Yang, H., X. Xie, M. Luo, and S. Jin, 2008, Target oriented full-wave equation based illumination analysis: 78th Annual International Meeting, SEG, Expanded Abstracts, 2216–2220. http://dx.doi.org/10.1190/1.3059326.

Yoon, K., and K. Marfurt, 2006, Reverse-time migration using the Poynting vector: Exploration Geophysics, **37**, 102–107. http://dx.doi.org/10.1071/EG06102.